Sustainable Energy & Fuels

# ETHANOL TO DIESEL: A SUSTAINABLE ALTERNATIVE FOR THE HEAVY-DUTY TRANSPORTATION SECTOR

| | |
|---|---|
| Journal: | *Sustainable Energy & Fuels* |
| Manuscript ID | SE-ART-10-2022-001377.R1 |
| Article Type: | Paper |
| Date Submitted by the Author: | 01-Dec-2022 |
| Complete List of Authors: | Restrepo Florez, Juan Manuel; University of Wisconsin-Madison, Chemical and biological engineering<br>Cuello-Penaloza, Paolo A.; University of Wisconsin-Madison<br>Canales, Emmanuel ; University of Wisconsin-Madison<br>Witkowski, Dustin; University of Wisconsin Madison,<br>Rothamer, David; University of Wisconsin-Madison<br>Huber, George; University of Wisconsin, Chemical and Biological Engineering<br>Maravelias, Christos; Princeton University, Chemical and Biological Engineering |
| | |

ARTICLE

# ETHANOL TO DIESEL: A SUSTAINABLE ALTERNATIVE FOR THE HEAVY-DUTY TRANSPORTATION SECTOR

Received 00th January 20xx,
Accepted 00th January 20xx

DOI: 10.1039/x0xx00000x

Juan-Manuel Restrepo-Flórez[a,b], Paolo Cuello-Peñaloza1[a], Emmanuel Canales[a], Dustin Witkowski[b], David A. Rothamer[b], George Hubber[a], and Christos T. Maravelias[c,d]

The combustion of middle distillates (diesel and jet fuel) is responsible for the emission of more than 2 GTon of $CO_2$ per year worldwide. While sustainable alternatives exist for gasoline and jet fuel, we still lack sustainable alternatives for diesel. This fact is especially relevant if we consider that electrification of sectors where diesel is used is challenging. One sustainable approach for diesel production is the catalytic upgrading of ethanol. While most work in this field has focused on the dehydration/oligomerization of ethanol, this approach is limited to producing fuels that have a high degree of branching and low cetane number. Another approach is the sequential use of ethanol Guerbet coupling, leading to higher alcohols, followed by etherification, leading to large ethers which, importantly, result in a product with high cetane number. In this work, we explore the catalytic upgrading of ethanol into diesel following an approach based on the initial Guerbet coupling of ethanol followed by etherification. The results presented are a collaborative and synergic effort among process and systems engineers, experimentalist in the area of catalysis, and fuel property modelers. We demonstrate experimentally the feasibility of upgrading ethanol into a diesel fuel with properties that surpass its fossil counterpart. The diesel produced has a predicted cetane number of ~70 and outstanding cold flow properties, while maintaining other properties (viscosity, density, and flash point) within expected ranges. A technoeconomic analysis performed based on a detailed biorefinery model shows that the MFSP is ~5.89$/Gal in 2021 dollars when lignocellulosic ethanol is used, with the most relevant economic driver the cost of the ethanol feedstock. The upgrading process can be performed with a net energy gain (EROI=1.49>1). An LCA analysis of greenhouse gas (GHG) emissions reveals that the use of lignocellulosic ethanol may lead to more than 50% reduction in GHG emissions compared to fossil diesel. Depending on the CO2 emissions associated with the production of ethanol we show that in some instances the production of carbon neutral diesel fuel is possible.

## Introduction

The projected increase in the market share of electric vehicles[1] added to the expected rise in fuel efficiency[2] will lead to a reduction in the gasoline demand. In contrast, the consumption of middle distillates is surging, a trend that is expected to continue for the next thirty plus years[3] because air, terrestrial, and maritime freight, where most middle distillates are consumed, are difficult to electrify and their use is increasing[4,5]. Consequently, middle distillates will continue to play a prominent role in the 21st-century energy landscape. Paradoxically, the biofuel industry in the U.S. has focused on the production of ethanol, which is blended exclusively with gasoline[3,6]. In 2021, the United States produced 17 billion gallons of ethanol, almost an order of magnitude larger than biodiesel[6,7]. Other countries have followed a similar trend. For example, Brazil, the second largest biofuels producer, manufactured ~8 billion gallons of ethanol in 2021, with only approximately 1.8 billion gallons of biodiesel[8,9]. Ethanol capacity will increase even more if lignocellulosic ethanol production plants are established[10]. This landscape can become challenging for two reasons. First, the sustainable alternatives for middle distillates, critically needed to mitigate climate change, are scarce and their production capacity is low. Second, a reduction in gasoline demand may lead to a surplus of ethanol in the market if gasoline supply is stable. Furthermore, the most common renewable diesel fuels, biodiesel and green diesel, are produced from vegetable oils and animal fats[11]. These feedstocks have limited availability and are expensive on an energy basis (~0.042$/MJ)[12]. In contrast corn grain (0.01-0.023 $/MJ)[13], and lignocellulosic biomass (0.003-0.005$/MJ)[14] are between 1.8-4 and 8-14 times lower in cost , respectively, and are widely available.

One option to simultaneously tackle the aforementioned challenges is to catalytically upgrade ethanol into middle distillates[3,15]. This approach takes advantage of existing and developing ethanol production infrastructure while producing the biofuels for which there is a more urgent need. Furthermore, this technology may be pivotal in repurposing existing ethanol production infrastructure as we transition toward an electrified light vehicle fleet. Additionally, from an energy security perspective, the production of biomass

[a] Department of Chemical and Biological Engineering, University of Wisconsin–Madison
[b] Department of Mechanical Engineering, University of Wisconsin–Madison
[c] Department of Chemical and Biological Engineering, Princeton University
[d] Andlinger Center for Energy and the Environment, Princeton University
*These authors contributed equally to this paper
Electronic Supplementary Information (ESI) available: [details of any supplementary information available should be included here]. See DOI: 10.1039/x0xx00000x

derived fuels is advantageous as it reduces the vulnerability of the energy system to abrupt changes in oil prices. A diesel production approach based on the catalytic upgrading of ethanol can exploit the diverse chemistries and catalysts available to transform ethanol into a wide range of molecules with varied properties, from olefins to ethers[3,6,15,16]. From a business stand point, in the US the production of biofuels may take advantage of the renewable fuel standard program[17]. For example, benefits for the production of biomass-based diesel with more than 50% reduction in GHG have oscillated between 0.075-5.25$/gal[17]. Additionally, a temporary tax credit of 1$/Gal is also available[18]. Motivated by these advantages researchers have developed ethanol upgrading processes to produce drop-in jet fuel[3,19–25]. Although bioethanol-derived jet fuel only represents a small share of the fuel market, its use shows the potential of ethanol upgrading as a practical, scalable, and potentially profitable technology. Chemically, ethanol-to-jet fuel upgrading has relied on two approaches: (1) A single pot process in which dehydration and oligomerization occur simultaneously[19]. (2) A process in which dehydration, oligomerization, and hydrogenation occur sequentially[20]. While the upgrading of ethanol to jet fuel has been reported and a significant body of experimental work[3,6,21], techno-economic analysis (TEA)[19,20,22,23,26,27], and lifecycle (LCA) stuides[19,26,28,29] exist, there is a significant lag in studies where the upgrading of ethanol to diesel is studied[15,24,30–32].

In principle, upgrading ethanol into diesel can be accomplished by ethanol dehydration to ethylene, followed by a sequence of oligomerization reactions[24]. However, this approach has significant challenges. First, the distillate yield may be low, a consequence of the molecular size distribution characteristic of oligomerization catalysts[3]. Second, the formation of highly branched products in oligomerization reactions leads to fuels with low cetane number[33]. An alternative approach, based on Guerbet chemistry and etherification, has been suggested for the upgrading of ethanol into diesel. In this approach, ethanol is first transformed into higher alcohols using Guerbet chemistry, and then these alcohols are transformed into ethers[34,35]. This approach has significant advantages in comparison with other cases in which the final product consists mainly of paraffins, namely, the distillate yield is higher[34]; and more importantly, the chemical and physical properties of ethers of higher alcohols are advantageous in diesel production. Ethers with more than ten carbons have viscosity, density, flash point, and boiling range similar to fossil diesel[34,36]. Additionally, they have a very high cetane number (>100), making them ideal candidates for the production of high-quality diesel (for reference, in the U.S. the minimum cetane number for diesel is 40)[37]. A high cetane number may enable the design of engine operation strategies with lower $NO_x$ emissions[38]. This characteristic allows us to postulate the possibility of producing diesel by catalytically upgrading ethanol into a diesel fuel blend with advantages over its fossil counterpart. This is in contrast with biofuel production strategies in which molecules or blends with similar, rather than superior, properties to fossil fuels are pursued.

In this work, we study the catalytic upgrading of ethanol to diesel based on Guerbet coupling and etherification. In this process, ethanol is transformed into higher alcohols which are then converted into a high cetane number ether blend. Minor olefin by-products are oligomerized. Bench-scale laboratory results, techno-economic analysis (TEA), and lifecycle analysis (LCA) are used to demonstrate the feasibility of transforming ethanol into a high cetane number diesel in a cost-effective and environmentally sustainable process. The results presented are the outcome of an iterative and collaborative effort between experimentalists, fuel property modelers, and process systems engineers. This synergistic collaboration has allowed us to tailor the experiments performed based on process modeling needs while ensuring that the fuels produced display desirable properties. Specifically, we provide accurate estimations of the macroscopic properties of the fuels produced (viscosity, density, low heating value, distillation curve, flash point, cloud point, and cetane number) and we show how the diesel produced can be used as a fossil diesel substitute.

## Technology overview

The ethanol upgrading approach envisioned in this work relies on three technologies: ethanol Guerbet coupling, higher alcohol etherification, and olefin oligomerization. In Figure 1, a schematic representation of the proposed refinery is presented, as well as the connections among the technologies employed and the main chemical components present in the connecting streams. At a high level, anhydrous ethanol is fed to the system and transformed into higher alcohols (C4+) using Guerbet coupling. These alcohols are subsequently transformed into ethers in an etherification reaction. Both of these reactions produce a small fraction of low molecular weight olefins as byproducts. Because of their size, these olefins are unsuitable to be used in diesel. To alleviate this limitation, the olefins are oligomerized to increase their average molecular weight. The biorefinery produces primarily diesel. The other by-products include: gasoline, which is produced with suitable low molecular weight species that cannot be blended with diesel; and steam, which is generated by burning low molecular weight paraffins (C2-C4), olefins (C2), and hydrogen. Steam produced in this way is used to partially offset the process energy needs.

**Guerbet coupling:** This reaction involves three mechanistic steps that all occur in one single reactor: (1) dehydrogenation of two alcohols to aldehydes, (2) aldol condensation, and (3) hydrogenation to form a higher alcohol[34,39]. Continued condensation of reaction products is possible, although in practice products with more than 12 carbons are rare with C4-C8 alcohols as the most abundant species. As noted by Eagan and coworkers[34], Guerbet chemistry is an oligomerization pathway that introduces branching in a more predictable way than olefin oligomerization. The main products of this reaction are higher alcohols. Byproducts include esters, olefins, aldehydes, ketones, and aromatics[34,39–43]. Additionally, a mole of water is produced per each mole of condensation reaction.

ARTICLE

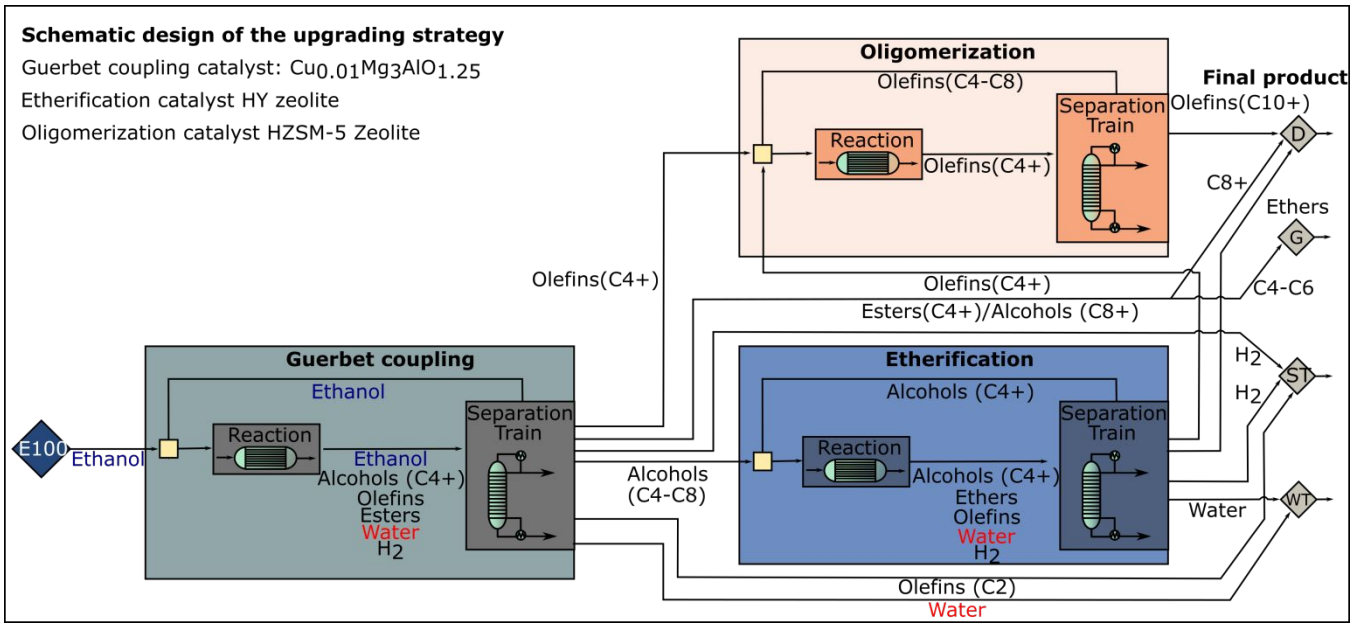


**Figure 1.** Schematic representation of an ethanol upgrading biorefinery based on Guerbet coupling, etherification, and olefin oligomerization. D: Diesel, G: Gasoline, ST: Steam, WT: Waste water.

Several heterogeneous catalysts can be used for the Guerbet coupling of ethanol[3,34,39,43–45]. These catalysts include hydroxyapatites[34,46], metal oxides[47,48], and decomposed layered double hydroxides[49]. The selection of the catalyst influences both conversion and selectivity. In this work, we use a Cu-based hydrotalcite-derived catalyst ($Cu_{0.01}Mg_3AlO_{1.25}$). This catalyst is stable for more than 100 hours[43]. Additionally, it has been shown that this class of Cu-based catalysts has a higher selectivity toward C6+ alcohols[43,50] in comparison with other catalysts commonly used in Guerbet reactions[42,51,52]

**Etherification:** The etherification of higher alcohols can be accomplished using acid catalysts[15,34]. In general, the product consists of a blend of ethers, olefins, and water[34,36]. The formation of olefins increases with temperature and with the fraction of branched to linear alcohols in the feedstock[34]. Available catalysts for this reaction include acid resins[34,53], alumina[54–56], and zeolites[53,57]. In this work, we use HY zeolite. This catalyst is both stable and commercially available at a low cost making it advantageous in future industrial applications. The selectivity of the catalyst was determined for different feed compositions as detailed in the methods section.

**Oligomerization:** Oligomerization of low molecular weight olefins is commonly used in the petrochemical industry[3,58,59]. Oligomerization reactions increase the average size of the molecules used as feedstock. The molecular weight distribution of the products is a function of the feedstock composition and the catalyst used. Typically, it follows a Schultz-Flory distribution[3,60]. The reaction conditions are a function of the composition, with C3+ olefins requiring milder conditions than ethylene[3,21,61]. Both homogeneous and heterogeneous catalysts have been used for these processes. In line with the principles of green engineering, we have selected a heterogeneous zeolite catalyst (HZSM-5) for this process[62]. The selected catalyst is known for producing a larger fraction of high molecular weight products, albeit their branching is usually high and their cetane number low[62,63]. We use this catalyst for the oligomerization of C3+ olefins. We have modeled the oligomerization reaction based on the data reported by Bond and coworkers[62].

## METHODS

**General approach:** To synergistically couple experimental studies and modeling, we follow the approach described in Figure 2:

(1) We use a set of Guerbet coupling experiments previously performed by some of the authors and partially reported with minor variations in Cuello-Peñaloza et al 2022[43]. These experiments were aimed at establishing the impact of ethanol conversion on selectivity.

(2) We use the results from the Guerbet experiments to inform process simulations of the Guerbet coupling area of the biorefinery. The main goal of these simulations is to determine the composition of the etherification reactor feed.

(3) We perform etherification experiments using the feed compositions determined. These experiments have as a main

ARTICLE

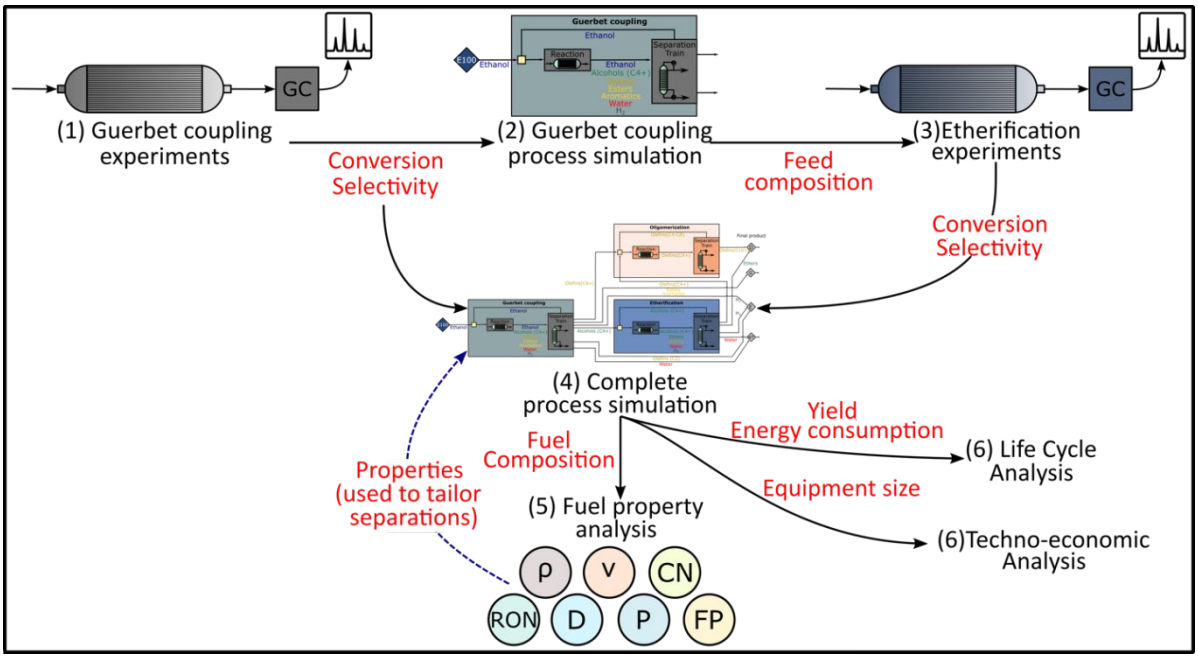


**Figure 2.** Approach followed in this work to couple experimental and simulation results. The flow of information at the different stages is shown in red fonts

objective to determine the conversion and selectivity obtained for the feeds of interests.

(4) Using the results both from etherification and Guerbet coupling experiments we perform a full plant simulation (Guerbet coupling, etherification, and oligomerization). This simulation allows us to calculate the final product composition (diesel) as well as the size of the equipment used in the biorefinery.

(5) With the composition resulting from the full plant simulation we analyze the properties of the fuels produced. If necessary, the separations within the plant are adjusted in an iterative manner to tailor the final products such that they meet ASTM standards[64,65].

(6) Finally, once the properties of the fuel products have been established, we perform TEA and LCA to determine the minimum fuel selling price (MFSP) and greenhouse gas (GHG) emissions.

Simulations are based on experimental results. Specifically, both the stoichiometry and the operational conditions in the process simulations are the same as those in the experiments.

**Etherification experiments:** The etherification of alcohol streams is carried out in an upward configuration flow reactor (33-cm long, 17.8-cm catalyst bed, 0.95-cm outer diameter) made of stainless-steel. The reactors are packed with 1.6-1.8 g (WSHV = 0.54-0.61 $h^{-1}$) of powder HY catalyst (Si/Al = 30) obtained from Zeolyst International and mixed with 30-80 mesh silica chips (Sigma Aldrich) in a 2:1 inert to catalyst mass ratio to minimize pressure drop. Model feedstocks are made in house and fed with a syringe pump (Eldex) at 0.02 mL/min, with Ar gas cofeed at 10 mL/min. Products flowing out of the reactor are crashed through a removable 140 mL glass condenser (ace glass) in a cold ice bath. Gases which do not condense are sent to a three-way valve positioned to flow through a bubble meter, gas bag or vent. Gas and liquid samples are collected simultaneously every 3 – 5 hours, with overnight samples being collected every 16-22 hours. The outlet flow of the reactor is redirected from the produce collection to a waste condenser when collection is conducted and switched back when a new condenser is placed. To reduce sampling error due to low product volumes, 1.46 mL of 1-heptanol is generally added to the condenser prior to collection. After collection, the sample mass is weighed, and the liquid is diluted with tetrahydrofuran (THF) with twice the predicted collected volume to ensure both the organic and aqueous phase are analyzed. The liquid is then diluted with THF including a known amount of 1-pentanol as an internal standard.

**Analytical techniques:** The reaction products for etherification are analyzed and quantified via GC-FID (Shimadzu 2014) equipped with a RTX-VMS column (Restek). Products are quantified with GC-FID via external standards when reference compounds can be obtained. When they cannot, response factors are estimated via the effective carbon number method. Products are identified via external standards when available, or via GC-MS suggestions. Gas bags are

used to collect the gases and these are analyzed in the aforementioned gas GC equipment configuration. In cases in which no standards are obtainable, e.g. for cross-etherification products, equimolar batch reactions are conducted to identify the retention times for said products. The batch reactor data is overlapped with continuous flow data to identify cross-etherification products, in which then effective carbon number theory is either used, or a standard of the same carbon number is obtained.

**Techno-economic analysis:** Capital costs and direct operating costs are estimated based on processes simulations performed in Aspen Plus V.10®. These simulations are set based on the experimental results. For the full plant integrating Guerbet chemistry, etherification, and oligomerization, Aspen Energy Analyzer is used to perform heat integration based on pinch analysis[66] and to design a heat exchanger network. The MFSP of diesel is determined by applying a discounted cash flow analysis. A facility able to process 176.4 MTon/year (~60MMGal/year) of anhydrous ethanol is designed. We assume 30 years of operation, as well as 40% equity and a 10-year loan at an 8% interest rate for financing. A discount rate of 10% and a 21% income tax rate are used. The economic parameters, biorefinery size, and installation factors used correspond to those reported in the most recent NREL report for lignocellulosic ethanol production[67]. All values are calculated in 2021 USD (See SI-1 for more details). The cost of the catalysts is determined based on commercial data for zeolites (etherification and olefin oligomerization), and it is calculated using the recently develop tool CatCost® for the Guerbet catalyst[68] (See SI-2).

**Life cycle analysis:** LCA is performed to understand the GHG emissions associated with the designed process. We are interested in the global warming potential (g $CO_2$-eq). The TRACI 2.1[69] methodology is used to determine the impact factors and GaBi® is used to model the process. The results are presented using MJ of fuel as a functional unit. A cradle to grave analysis is performed where the end use phase is modelled assuming that all carbon contained in the fuel is transformed into $CO_2$. The system boundary includes the following processes: lignocellulosic feedstock production and transportation, ethanol production from lignocellulosic residues, ethanol upgrading, fuel transport, distribution, and fuel combustion. The main product of the upgrading process is diesel (#1 and #2), to account for the co-production of gasoline we use the displaced burden method[70]. Some of the byproducts are used to offset the energy needs of the refinery (i.e., the energy obtained from the combustion of energy rich by-products in ethanol upgrading). Life Cycle Inventories (LCI) for ethanol upgrading are established based on the process simulations in this work. For the emissions associated with lignocellulosic ethanol production, we use a range of values representative of current literature[29,71,72]. For other processes the LCI is established based on the energy database from GaBi®.

**Fuel property analysis:** Models from the literature were used to calculate relevant physical properties of the fuel blends produced in this work. Density was calculated using a linear by volume mixing rule[73,74]. Liquid kinematic viscosity was calculated using the UNIFAC-VISCO method[75]. The flash point was modeled using the mixing rule of Liaw and coworkers[76]. Flash point data for each component was used where available and supplemented with predicted flash points for individual components using the group contribution model of Carroll and coworkers[77]. The cloud point of the fuel blend is treated as the thermodynamic equilibrium boundary temperature between the one-phase (liquid) and two-phase (solid/liquid) region for the fuel mixture[78]. Similar to the cloud point, the distillation curve for each blend was calculated as a thermodynamic equilibrium between the liquid and gas phase[79]. Finally, the derived cetane number (DCN) was estimated using an autoignition model that incorporates group contribution methods to calculate global initiation and chain branching rate constants for each component in the blend[80]. The model was recently developed to provide accurate DCN estimates for oxygenated components and blends with wide ranges of individual cetane numbers, where linear by volume mixing rules are no longer sufficient. Further details see supplemental information (SI-5).

## RESULTS

### Guerbet coupling

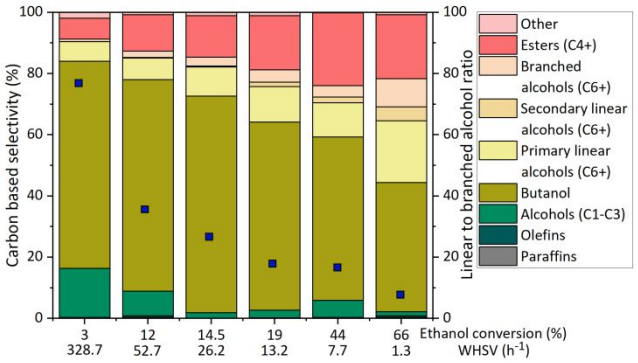


**Figure 3.** Product distribution as a function of ethanol conversion in a Guerbet coupling reaction performed using $Cu/Mg_xALO_y$ as catalyst. The linear to branched alcohol ratio is indicated by a blue square (defined as the ratio of the carbon selectivities of linear to branched alcohols). In the reaction, aldehydes and ketones are also produced, these species are accounted for by lumping them with their respective alcohols since they can be easily hydrogenated to form their parent alcohols, for example using a dual bed catalyst. The data is based on the report by Cuello-Penaloza et al[50].

*Experimental results:* The product selectivity in the Guerbet coupling reaction as a function of ethanol conversion is shown in Figure 3. This data is partly based on experiments reported by Cuello-Penaloza et al[50]. At low conversion (e.g., 3% and 12%) low molecular weight alcohols (C1-C4) are the most abundant products. As the conversion increases so does the fraction of higher alcohols (C6+) and esters (See SI-3 for a detailed product composition). The increase in higher alcohols (C6+) is important in the context of diesel production by etherification. We note that the production of esters, secondary alcohols, and branched alcohols can be regarded as undesirable. Esters cause undesired reactions during etherification (see etherification section), while branched and secondary alcohols are more prone to form olefins instead of ethers[34]. Since the production

ARTICLE

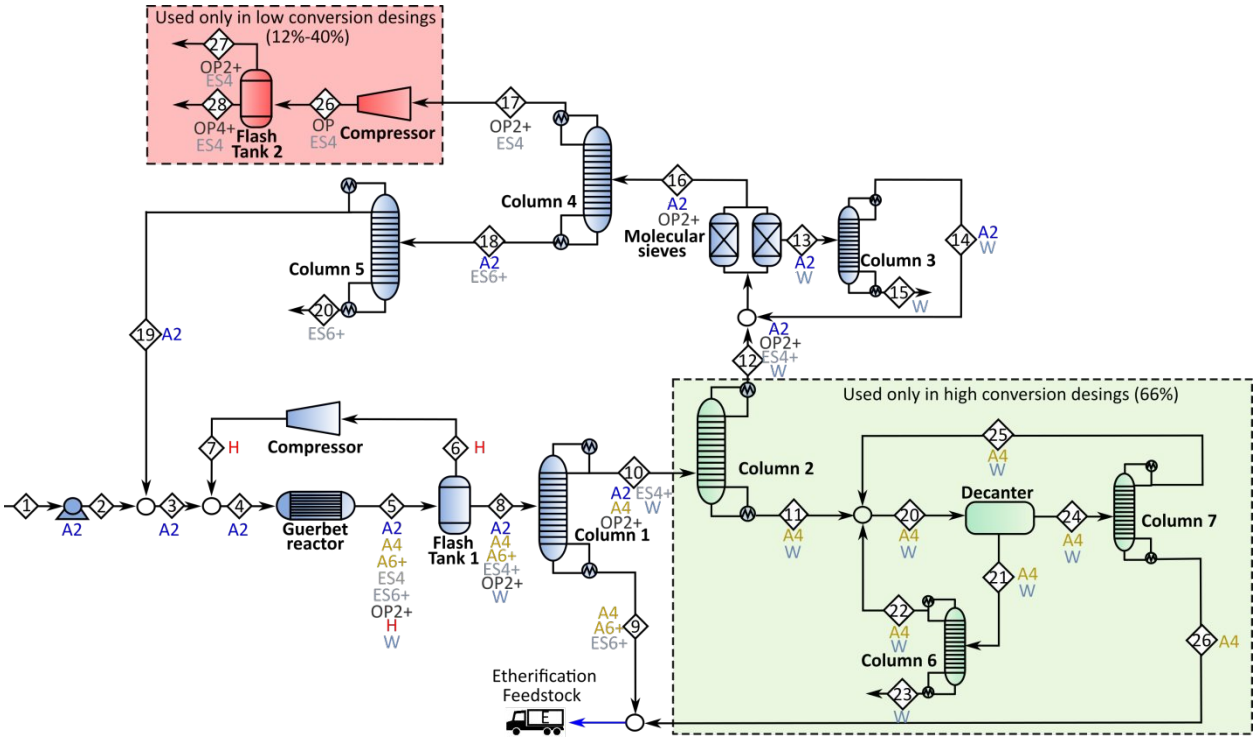


**Figure 4.** Layout for the Guerbet coupling area. Operations inside the green square (Heteroazeotropic distillation of 1-butanol) are used only at high conversion (66%), while those in red are only used at low conversions (12%-40%). Chemical species are labeled such that A: Alcohols, ES: Esters, OP: Olefins/Paraffins, H: Hydrogen, and W: Water, the numerical characters indicate the carbon length. The blue stream is the one containing all the higher alcohols which serve as the feed to the etherification area.

of esters and secondary alcohols increases with conversion, and the ratio of linear to branched alcohols diminishes (Figure 3), then a trade-off appears. Higher conversions are desired because they lead to the production of larger alcohols, require equipment with lower size, and usually consume less energy in pumping and separations because the streams associated are smaller. However, at these higher conversions more undesirable products are obtained.

*Process modeling*: Using the experimental results obtained for Guerbet coupling, we synthesize process layouts for conversions between 12%-66% (Figure 4). The 3% conversion is too low to be economically relevant so was not used in this analysis. We study how conversion affects: (1) the process configuration; (2) the composition of the stream fed to the etherification reactor (note that this is different from the results discussed in Figure 3 because the effect of separation operations in now considered); and (3) the capital and operating costs of the Guerbet coupling area.

The process configuration is shown in Figure 4. The Guerbet reactor is followed by a flash tank that allows recycling of the carrier gas. Once the carrier gas is removed, a distillation column (column 1) is used to recover unconverted ethanol as the top product, while keeping an anhydrous blend of higher alcohols (C4+) as the bottom product. For low to moderate conversion (12%-44%), all the butanol produced remains in the bottom product of distillation column 1. At high conversion, a fraction of the butanol is obtained in the top product, thus for high conversion (66%), 1-butanol heteroazeotropic distillation is required to separate ethanol, butanol and water before recycling. These results are consistent with the results of Nezam and coworkers[41]. A molecular sieving unit is used to remove the remaining water from the recycle stream. Finally, two distillation columns (columns 4 and 5) are used to remove esters and olefin byproducts. At low conversion, column 4 operates under vacuum and a compressor is required, this compressor is followed by a flash tank to remove low molecular weight olefins and paraffins.

In Figure 5, we show the annual operating costs (Figure 5(a)), capital costs (Figure 5(b)), and composition of the stream used for etherification (Figure 5(c)) as a function of conversion. As expected, both capital and operating costs are significantly reduced when the

ARTICLE

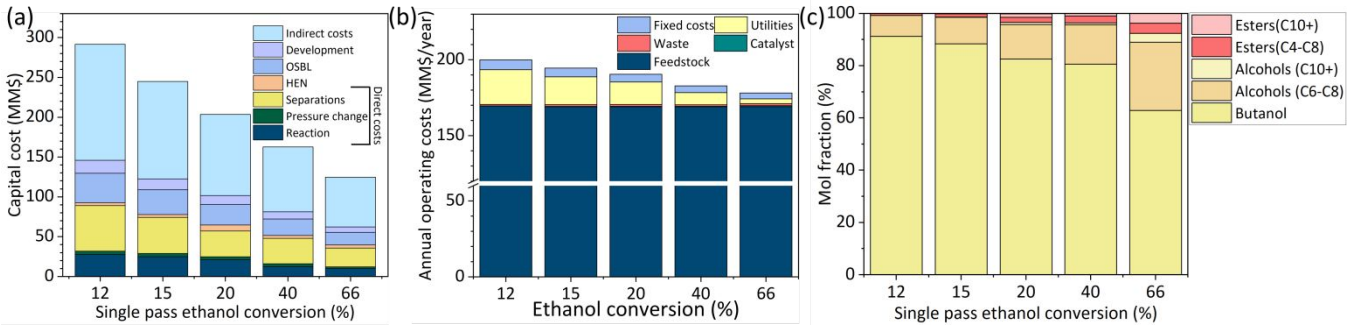


**Figure 5.** (a) Capital costs (b) annualized operating costs (c) and composition of the etherification feed stream as a function of conversion for the Guerbet coupling area. Details on the capital costs and operating conditions can be found in SI-4

conversion increases; e.g., when conversion increases from 12% to 66% capital costs are reduced by ~50%, and operating costs by ~10%. For capital costs, separations play the most prominent role. For operating costs, feedstock is the most important factor; although utilities are also significant. When conversion increases from 12% to 66% the cost of utilities is reduced ~7 times (from ~20MM$/year to ~3MM$/year). This result is important for sustainability because lower utility consumption leads to lower environmental impact. The composition of the stream fed to the etherification area is also significantly affected by conversion (Figure 5(c) and SI 6). At low conversion, this stream contains mainly 1-butanol with a small fraction of C6+ alcohols and an almost negligible amount of esters. While at high conversion, a larger fraction of C6+ alcohols and esters are present. For reference, 1-butanol composition drops from ~90% to ~60% when the conversion increases from 12% to 66%. In parallel, higher alcohol content in the etherification feed stream increases from ~8% to ~30%, with a concurrent increase in esters from 0.7% to 7.5%. We note that low molecular weight olefins, C1-C3 alcohols, water, and a significant fraction of C4-C6 esters have been removed from the reactor outlet stream by means of separation operations in the Guerbet area.

**Etherification**

*Experimental results:* Since the alcohols used in etherification are those produced in the Guerbet area, we prepare two representative feed streams resembling the composition obtained at low (12%) and high (66%) single-pass ethanol conversion in the Guerbet area (see Figure 5(c)), we refer to these feeds as G-12% and G-66%, respectively. First, we are interested in establishing if the presence of esters in the reaction feed affects product selectivity. To address this question, we use the G-12% feedstock which is simpler. We perform etherification of this feedstock under two conditions: (1) we assume that the G-12 stream contains a mol fraction of esters of ~1% (ethyl butanoate 15%, butyl acetate 63%, and ethyl hexanoate 22%) and (2) we assume that no esters are present in the reaction. We observe that the carbon balance of the reaction drops from 96% to less than 90% when esters are present in the reaction feed stream (see SI 7), indicating that esters may lead to the formation of undesirable products. This result points toward the need to remove as much of the esters as is economically possible from the etherification reactor feed.

Second, we are interested in understanding how the composition of the etherification reactor feed affects the product distribution. Considering that esters may affect the carbon balance, we perform these experiments in their absence. Both the feed and product composition of the etherification reaction are shown in Figure 6(a). For the G-12% feed, which is richer in 1-butanol, the main product is di-n-butyl ether, with minor quantities of larger ethers (C10+), and low molecular weight olefins. On the other hand, for the G-66% feed, a larger fraction of ethers with more than 10 carbons is formed; however, more olefin by-products are obtained as well. In the etherification reaction, multiple alcohols are present in the feed. Each of these alcohols participates in different reactions. Consequently, the original carbon contained in each alcohol is distributed among the products that result from the reactions in which the alcohol is involved. In Figure 6(c), we show how the carbon contained in each alcohol is distributed among four types of products: di-n-butyl ether, ethers with more than 10 carbons, olefins, and what is labelled as unassigned carbon (UA), where we group products that were detected by the analytical techniques used but whose identity is unknown. In general, β-branched and secondary alcohols lead mainly to the formation of olefins. In contrast, linear primary alcohols lead predominantly to the production of ethers. We note that the fraction of carbon used for the production of unidentified species is large for some alcohols (e.g., A5), however the alcohols for which this is the case are present in the feed at low concentration, such that the overall fraction of unidentified species is only ~5%.

ARTICLE

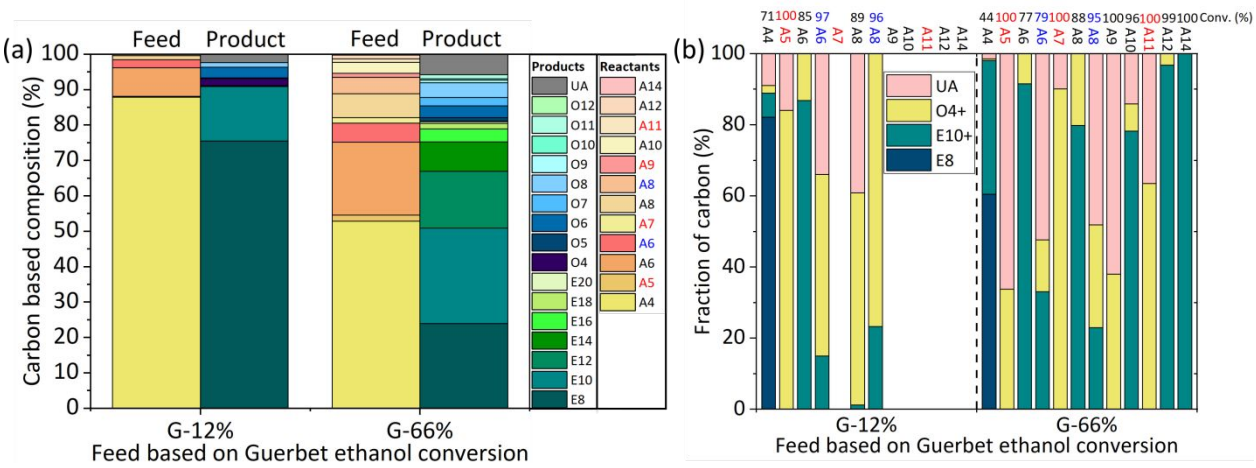


**Figure 6.** Experimental results obtained for different etherification reaction conditions (a) feed and product composition in the etherification reaction when G-12% and G-66% feeds are used (b) carbon selectivity for each alcohol in the feed for the G-12% and G-66% reactor feeds. The conversion as a % of carbon is shown above for each alcohol. Chemical species in the figure are labelled using the following convention: a letter indicates the functional group (A: alcohols, O: olefins, E: ethers, UA: Unidentified components), and a numerical character the carbon length. Additionally, for alcohols we use a color code, such that linear alcohols are shown in black, secondary alcohols in red, and branched alcohols in blue.

*Process modelling:* Di-n-butyl ether is the primary product obtained when a G-12% feedstock is used in etherification (Figure 6(b)). In contrast, when a G-66% feedstock is used, a smaller fraction of di-n-butyl ether is produced with a concomitant increase of ethers with more than 10 carbons. Considering that di-n-butyl ether has a flash point significantly lower than diesel #2 (~25°C vs 52°C), we use the G-66% feedstock for the rest of this work. Consequently, we synthesize an etherification area to process this feedstock (Figure 7). At a high level, the unit operations in this area can be divided into a preconditioning sub-area and a reaction/separation sub-area. In the preconditioning sub-area, the ester content of the feed stream to the etherification reactor is reduced to less than 0.3% (mol/mol). The reaction/separation area consists of a reactor, and a sequence of unit operations that enable recycling unconverted alcohols while simultaneously obtaining relatively pure ether streams that will be used in the final diesel blend. We have made the design decision to not feed alcohols with ten or more carbons to the etherification reactor (see distillation column 3). These alcohols are large enough to have physiochemical properties compatible with diesel so that they can be blended directly into diesel fuel. They are also in small enough quantities to not cause concerns with the melting point of the fuel blend. Removing them in the preconditioning sub-area before etherification allows us to reduce the ester content of the etherification reactor feed to less than 0.3% (mol/mol)

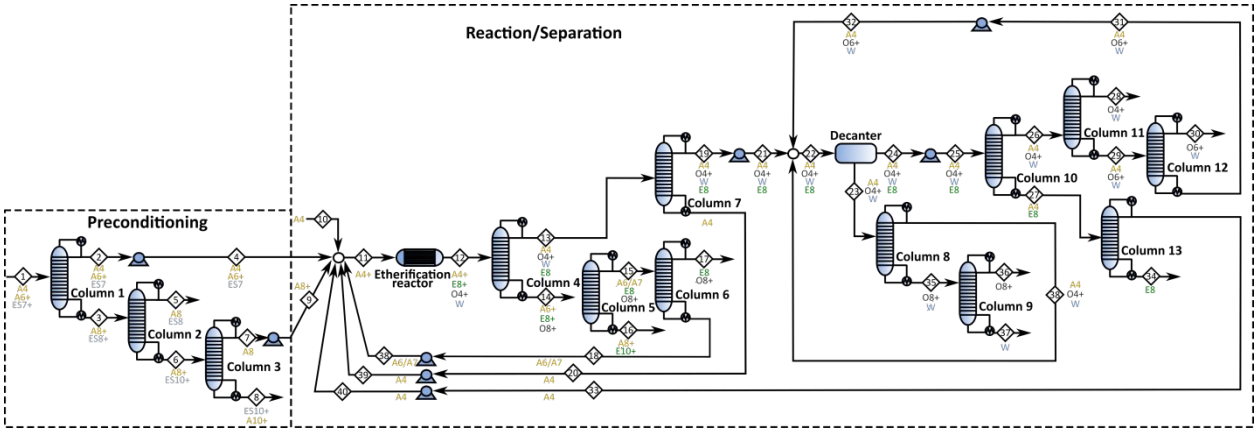


**Figure 7.** Layout for the etherification area. Chemical species in the figure are labelled using the following convention: a letter indicates the functional group (A: alcohols, O: olefins, E: ethers, UA: Unidentified components), and a numerical character the carbon length.

ARTICLE

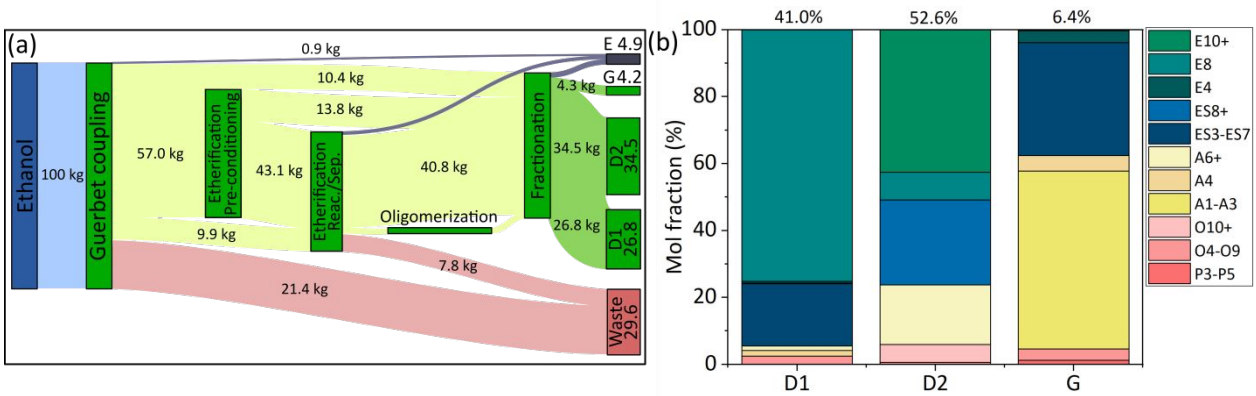


**Figure 8.** (a) Sankey diagram with the mass flows within the biorefinery. Yellow arrows represent material flows of fuel precursor elements, red arrows waste streams, blue arrows by-products used in electricity production, and green arrows fuel streams (D1: diesel #1, D2: diesel #2, and G: Gasoline). (b) composition of the fuels produced. Chemical species in the figure are labelled using the following convention: a letter indicates the functional group (A: alcohols, E: ethers, ES: esters, O: olefins, and P: paraffins), and a numerical character the carbon length.

*Process modelling and fuel characterization:* Using the results obtained from both Guerbet coupling and etherification, we synthesize a biorefinery for the upgrading of ethanol into diesel following the approach shown in Figure 2. For this design we use the experimental data (Figures 3 and Figure 6) for G-66% from the Guerbet step and etherification steps. A Sankey diagram showing the mass flows within the biorefinery is presented in Figure 8(a). A total fuel yield of ~65 wt% is obtained. This fuel is fractionated into three main products: diesel #2 (52.6%), diesel #1 (41.0%), and gasoline (6.4%). The composition of these fuel fractions is shown in Figure 8(b). In the case of diesel, the product is dominated by ethers, but the presence of other molecules (esters, alcohols, and olefins) produced by the catalytic reactions used is also significant. We note that the diesel #2 blend is richer in ethers with more than 10 carbons, while the diesel #1 blend is constituted mainly of di-n-butyl ether (~75%). The gasoline fraction on the other hand, consists of low molecular weight components obtained in the Guerbet and etherification areas (methanol, ethanol, esters, and olefins). We estimate the properties of these fuels and compare them with respect to the ASTM standard[64,65] (Figure 9). For diesel #2, all properties are close to those of a typical fossil diesel, with a cetane number significantly higher than the minimum required (73 vs. 40)[64].

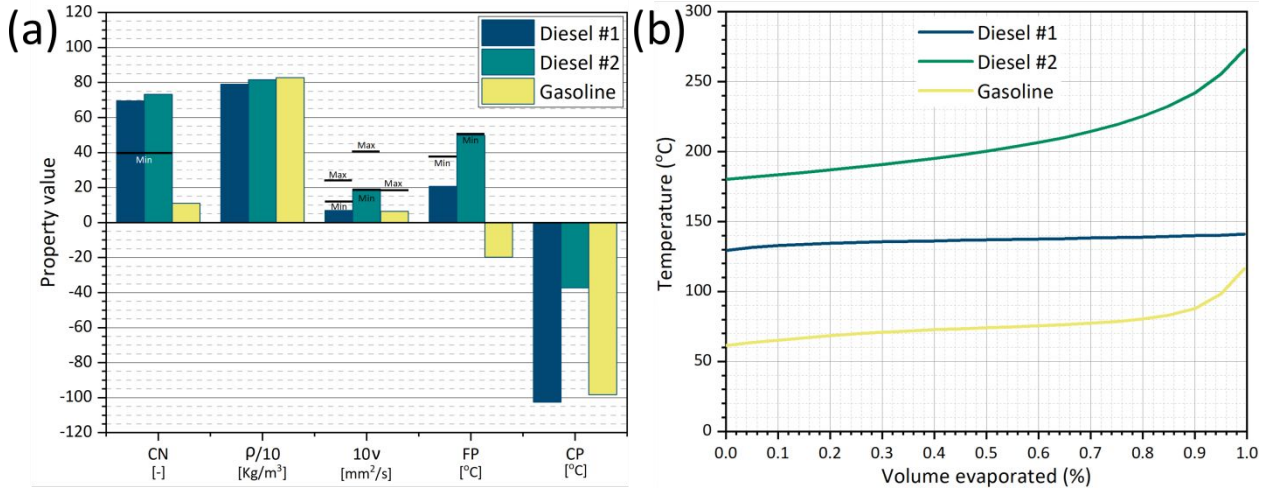


**Figure 9.** (a) Properties of the different fuels produced. CN: cetane number, D: density, V: viscosity, FP: flash point, CP: cloud point. The ASTM requirements for the properties that are constrained are indicated by horizontal black lines (b) Distillation curve of the fuels produced.

ARTICLE

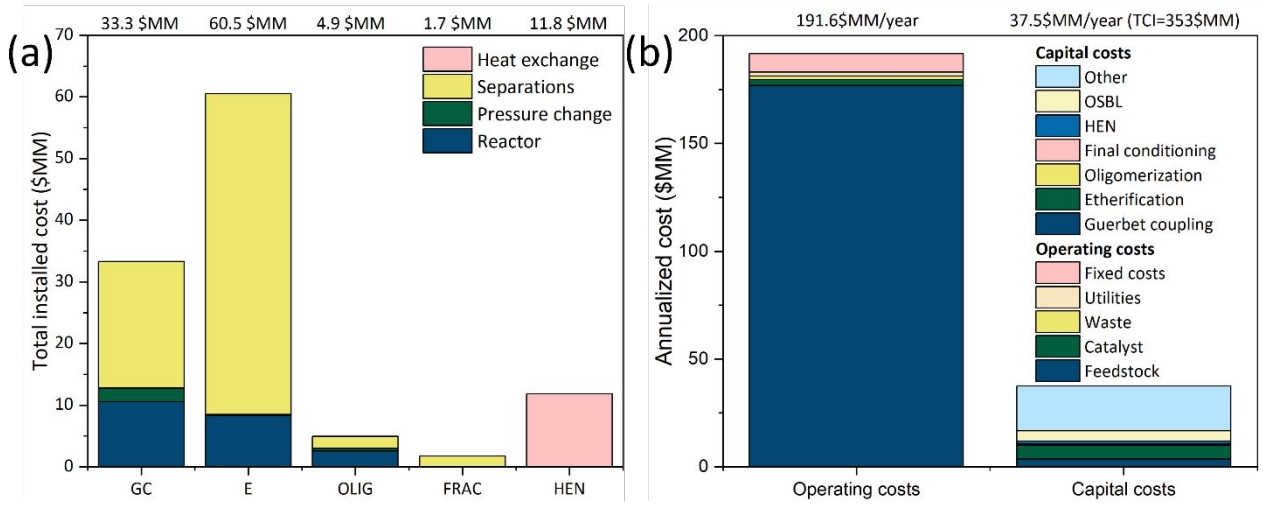


**Figure 10.** (a) Installed capital costs of the different areas in the biorefinery (b) Annualized capital and operating costs. GC: Guerbet coupling, E: etherification, OLIG: oligomerization, FRAC: fractionation, HEN: heat exchanger network, OSBL: outside battery limits.

This result is promising and suggests that the proposed catalytic approach can lead to the production of biofuels with superior properties. Both the density and viscosity of diesel #2 fall within the expected range, and the flash point is only slightly under the standard (50°C vs 52°C). This result is not limiting considering that the initial boiling point of the produced diesel #2 (closely related to the flash point) can be increased, if needed. For example, the distillation conditions can be modified to increase the initial boiling point with only a minor impact on fuel yield. The cold flow properties of diesel #2 are outstanding, with a cloud point of ~-37°C, such that it could be used as a winter fuel. The diesel #1 obtained presents a lower flash point (~21°C vs 38°C) and viscosity (~0.7 °mm$^2$/s vs 1.3 mm$^2$/s) than the ones required in the ASTM standard[64]. This implies that the produced diesel #1 can only be used in blends and not as a drop-in biofuel. Finally, the gasoline fraction satisfies the viscosity requirement[65], and has an estimated RON value (based on the cetane number) of ~99. The distillation curve of the produced fuels is shown in Figure 9(b). In all cases, the fuels boil in the expected range. However, for diesel #2, we have a T90 that is lower than the ASTM requirement (241°C vs 288°C for diesel #2). The fact that our diesel #2 has a lower T90 may impact the fraction that can be blended with a fossil diesel. However, from an operational standpoint there is good evidence that having a lower T90 does not impact engine operation and may actually be beneficial considering that the diesel #2 produced satisfied the flash point requirements[81]. We note that for diesel #1, the curve is very flat which is explained by the fact that this fraction is mainly constituted of di-n-butyl ether. The properties of the fuels produced are similar to those of fossil diesel; therefore, they are suitable to be used in heavy duty transportation applications such as trucks and ships.

*Economics:* The installed capital costs associated with the different biorefinery areas are shown in Figure 10 (a). The Guerbet and etherification areas have the higher capital costs, and within them, the capital cost of separation units is dominant. It is noteworthy that the HEN also has a significantly high capital cost. The total capital investment is estimated at ~353 $MM. The annualized capital and operating costs are shown in In Figure 10(b). Operating costs are dominant, with the cost of feedstock been the most important component. We assume that the ethanol upgrading plant is installed as an extension of a lignocellulosic ethanol production plant that operates as described in the most recent NREL report[67]. Under this assumption, the energy by-products obtained in the ethanol production plant can be used to satisfy the energy needs of ethanol upgrading. The economic analysis reflects this assumption.

Figure 11(a) shows the breakdown of the minimum selling price which was calculated to be equal to 5.89 $US/Gal (7.68 $/GDE). We used an ethanol price of 2.98$/Gal, which is the MFSP estimated for ethanol from corn stover when all by-products in ethanol production are used within the process and no credits for electricity sales are obtained[67]. Alternatively, if we use an ethanol price of 1.75 $/Gal (the average corn grain ethanol price in the last 10 years)[82] we obtain a MFSP of 4.06$US/Gal (5.29$/GDE). The sensitivity of the MFSP to different parameters is shown in Figure 11(b), where the parameters are grouped into three categories: parameters related to capital costs, parameters related to operating costs, and financial parameters. The plot shows the percentual change in the MFSP (x-axis) when the parameters in the y-axis change between the limits shown at the left and right side of each bar (e.g., when the price of ethanol is 1$US/Gal, the MFSP is reduced by ~40%). The range selected for each parameter reflects plausible possible

ARTICLE

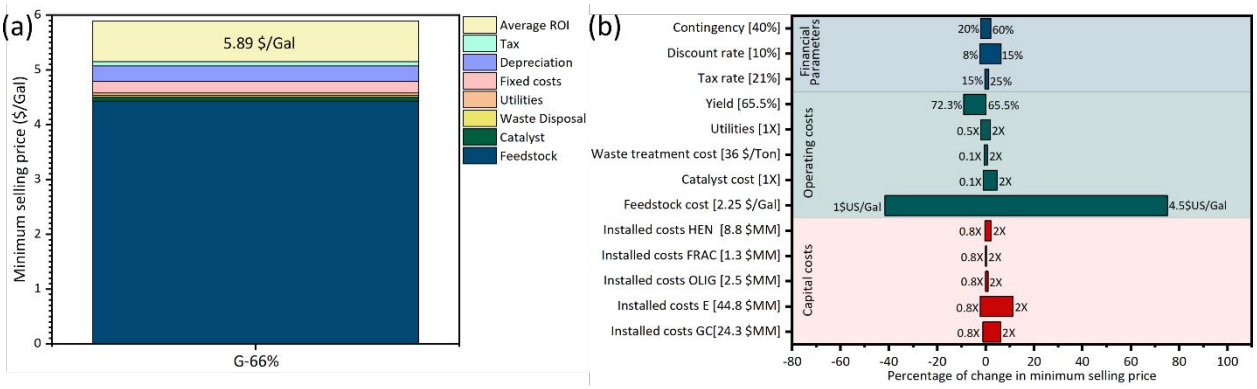


**Figure 11.** (a) Breakdown of the MFSP (b) tornado plot showing the sensitivity of the MFSP to changes in different parameters of interests (y-axis). The value within the bracket on the y-axis represents the value of the parameter in the reference case. GC: Guerbet coupling, E: etherification, OLIG: oligomerization, FRAC: fractionation, HEN: Heat Exchanger Network.

improvements in the design, or the possibility of having overoptimistic assumptions in our analysis. For comparison, the estimated production cost of traditional biodiesel obtained by the transesterification of fatty acids has ranged between 3.92-6.00 $/GDE[83]. Additionally, since traditional biodiesel is mostly produced from vegetable oils it has the disadvantage of directly competing with food. Other technologies to produce biodiesel, like fast pyrolysis, show the potential to have lower production costs (~3.03-4.54 $/GDE) while eliminating the competition with food. However, in these cases the properties of the fuels produced cannot be precisely tailored like in the ethanol to diesel approach described here.

The sensitivity analysis reveals that the capital costs of the Guerbet and etherification areas are the most important parameters related to capital costs. The cost of feedstock and the fuel yield are the most important parameters related to operating costs. Finally, the most important financial parameter is the discount rate. These results point toward two research directions. First, designing more less capital-intensive separation trains may be important especially in the Guerbet and etherification areas. Second, designing more selective catalysts leading to the formation of smaller amounts of by-products may improve the fuel yield. Finally, since the MFSP is heavily dependent on the ethanol cost, finding strategies to produce cheaper ethanol (e.g. by using high value low volume co-products[84]), will have a direct impact on the MFSP of diesel.

*Energy analysis*: A Sankey diagram with the energy flows within the biorefinery is shown in Figure 12(a). These energy flows have been normalized to those required to process 100MJ of ethanol. Efficiency factors have been used to ensure that these flows represent energy of the same "quality". Boiler efficiency is assumed to be 80%. Additionally, an overall energy balance in the ethanol production plant is used to determine the LHV of the biomass used to produce excess electricity[67]. The figure reflects the utilization of excess energy generated in ethanol manufacture and upgrading to satisfy the refinery energy needs. The biorefinery area that consumes the largest amount of energy is Guerbet coupling (25.1 MJ), followed by etherification (21.8 MJ). The energy consumption in these areas could be reduced if a simpler separation train is developed. Considering that the main group of by-products consists of esters, which need to be removed before etherification, it would be important to develop either catalysts or processes leading to a reduction of these components. For example, if no significant amounts of esters are produced, then the whole pre-conditioning sub-area could be avoided, saving approximately 5.8 MJ of energy.

The estimated energy return on investment (EROI) of the biorefinery is ~1.49. The EROI is defined as the ratio between the energy produced by a process and the energy required to produce/extract that energy[85]. Since the EROI>1, we have a net energy gain. However, the EROI value is low, considering that typical fossil fuels have an EROI ~20, and that a value close to 3 has been suggested as a minimum for a fuel in a sustainable society[85,86]. To understand the effect that technological improvements may have on the EROI we perform a sensitivity analysis (Figure 12(b)). We analyze two factors: the cumulative energy consumed during the upgrading process (x-axis), and the cumulative energy used in the production of the ethanol feedstock used (y-axis). Improving either of them will have a significant impact on the biorefinery's EROI. For reference, if no improvement in ethanol manufacture is achieved but the energy consumed during ethanol upgrading is reduced by ~50%, the EROI increases to ~2. The same improvement can be obtained if no improvement in ethanol upgrading is achieved but the energy used

ARTICLE

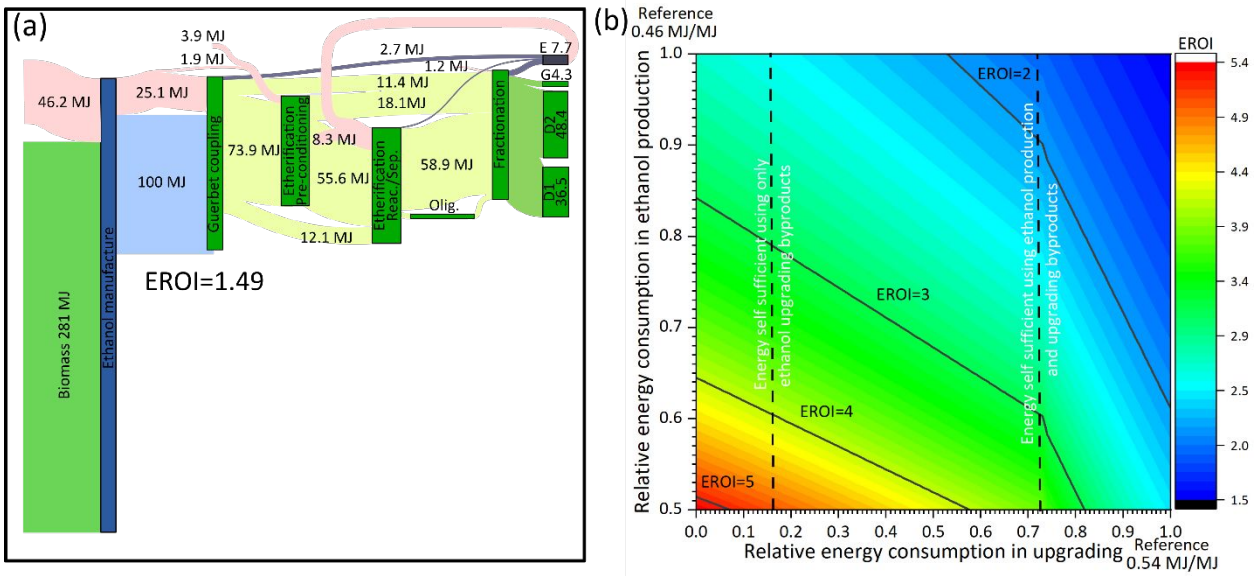


**Figure 12.** Energy analysis of the ethanol upgrading biorefinery (a) Sankey diagram showing energy flows (LHV) within the biorefinery (b) Sensitivity analysis showing the EROI value as a function of the energy consumed in ethanol production (y-axis), and ethanol upgrading (x-axis), values are presented as relative values with respect to the reference. The vertical dashed line represents the reduction in energy consumption in ethanol upgrading that is required to obtain a self-sufficient refinery (i.e., a biorefinery in which the energy contained in the byproducts is sufficient to satisfy all energy needs). The energy flows in the figure correspond to the those observe when 100MJ of ethanol are processed.

in ethanol production is reduced by ~40%. A reduction in energy consumption in upgrading by 50% accompanied by a 30% reduction in the energy consumed in ethanol production lead to an EROI of ~3.

We emphasize that improvements in the upgrading energy consumption are contingent on the development of better catalyst, and simpler separation trains. On the other hand, reducing energy in ethanol production is possible if improvements in biomass productivity, and biomass preprocessing (drying, chopping, etc.) are achieved[87], or if the sustainable manufacturing of fertilizers is developed[88]. For example, increasing biomass yield by a factor of three in comparison with current practices may lead to reductions in energy consumption of ~15%. Likewise, reducing the energy in preprocessing depot facilities (from 750 MJ/Mg to 500 MJ/Mg) while increasing the densification factor (above 6) may lead also to ~15% less energy consumption[89]. Another avenue consists in reducing the energy expended in separations.

The estimated energy return on investment (EROI) of the biorefinery is ~1.49. The EROI is defined as the ratio between the energy produced by a process and the energy required to produce/extract that energy[85]. Since the EROI>1, we have a net energy gain. However, the EROI value is low, considering that typical fossil fuels have an EROI ~20, and that a value close to 3 has been suggested as a minimum for a fuel in a sustainable society[85,86]. To understand the effect that technological improvements may have on the EROI we perform a sensitivity analysis (Figure 12(b)). We analyze two factors: the cumulative energy consumed during the upgrading process (x-axis), and the cumulative energy used in the production of the ethanol feedstock used (y-axis). Improving either of them will have a significant impact on the biorefinery's EROI. For reference, if no improvement in ethanol manufacture is achieved but the energy consumed during ethanol upgrading is reduced by ~50%, the EROI increases to ~2. The same improvement can be obtained if no improvement in ethanol upgrading is achieved but the energy used in ethanol production is reduced by ~40%. A reduction in energy consumption in upgrading by 50% accompanied by a 30% reduction in the energy consumed in ethanol production lead to an EROI of ~3. We emphasize that improvements in the upgrading energy consumption are contingent on the development of better catalyst, and simpler separation trains. On the other hand, reducing energy in ethanol production is possible if improvements in biomass productivity, and biomass preprocessing (drying, chopping, etc.) are achieved[87], or if the sustainable manufacturing of fertilizers is developed[88]. For example, increasing biomass yield by a factor of three in comparison with current practices may lead to reductions in energy consumption of ~15%. Likewise, reducing the energy in pre-processing depot facilities (from 750 MJ/Mg to 500 MJ/Mg) while

increasing the densification factor (above 6) may lead also to ~15% less energy consumption[89]. Another avenue consists in reducing the energy expended in separations.

**Environmental analysis**

In Figure 13, we analyze the GHG emissions per MJ of energy contained in the fuel as a function of the carbon intensity of the ethanol used as feedstock. We assume that energy by-products obtained in the upgrading process are used to satisfy the refinery energy needs. We note that a 50% reduction in GHG emissions in comparison with fossil diesel is attainable when the carbon intensity of the ethanol feedstock is below 14 g-CO2-eq/MJ-Ethanol; this value falls within the range commonly reported for lignocellulosic ethanol and sugar cane ethanol[90]. To obtain a carbon-neutral diesel fuel, ethanol with carbon intensity lower than -23.4 g-CO2-eq/MJ-Ethanol is required. This low carbon intensity falls into the range predicted in some studies for lignocellulosic ethanol. Alternatively, it could be obtained by implementing a carbon capture technology in the ethanol production process. In particular, capturing at the fermentation outlet is not energy intensive (~0.015MJ/MJ of ethanol[91]) provided that the composition of this stream is mostly $CO_2$. A reduction of ~33.6 g-CO2-eq/MJ-Ethanol could be attained by implementing $CO_2$ capture at this outlet[91,92].

Additional improvements in the upgrading process as the technology develops may lead to a reduction in the energy consumed, thus improving current estimates. For example, if the upgrading process can be done in an energy self-sufficient design (such that the energy in the upgrading coproducts is enough to satisfy all the upgrading energy needs), then it would be possible to reduce the energy consumption by more than 0.39 MJ/MJ of ethanol processed. For reference, common carbon intensities for lignocellulosic ethanol range between -29 to 70 g-CO2-eq/MJ-Ethanol depending on the assumptions made, geographic location, and impact factors for chemicals used in the process (e.g., corn steep liquor, ammonia, and glucose)[72,90,93,94]. Corn ethanol without $CO_2$ capture has carbon intensities from ~50 to 117 g-CO2-eq/MJ-Ethanol[90]. Finally, ethanol produced from sugar cane has carbon intensities reported from 9 to 55 g-CO2-eq/MJ-Ethanol[90].

## Conclusions

This works presents an integrated approach between experimental heterogeneous catalysis and process systems engineering towards the design of an ethanol upgrading biorefinery for the production of diesel. The fuels produced exhibit advantageous properties in comparison with their fossil counterparts, especially with respect to the cetane number (>70 for both diesel #1 and diesel #2) and cold flow properties (cloud point lower than -35 °C). The experimental results demonstrate the selective transformation of ethanol into higher alcohols, and the subsequent conversion of these alcohols to ethers of high molecular weight. Coproducts include olefins and esters. Systems engineering was used to first synthesize a process based on the experimental results, and then perform TEA and LCA. The produced diesel has an MFSP of 5.89 $/Gal (6.86 $/GGE), and, importantly, the process has a net energy gain (EROI=1.41>1). The analysis of the GHG emissions showed that if corn stover is used as feedstock, then a 50% GHG reduction is possible. Additionally, if the ethanol carbon intensity is sufficiently low, we demonstrate the possibility of obtaining carbon neutral diesel fuel. Future research in this area should focus on finding strategies that can lead to the simplification of the necessary separations and the development of more selective catalysts, as such improvements will have an impact on both the EROI of the fuels produced and GHG emissions.

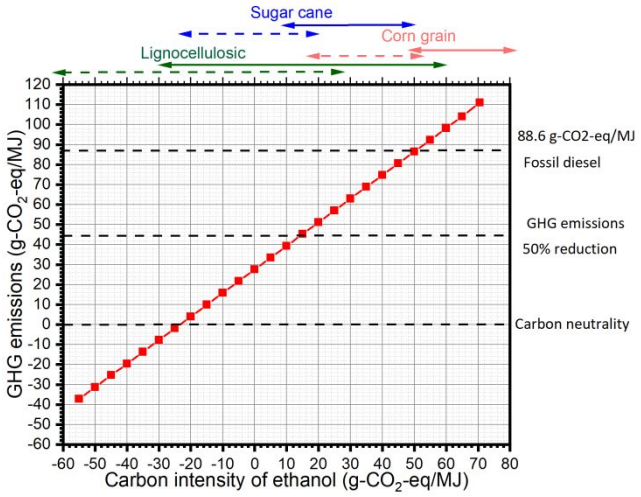


**Figure 13.** Greenhouse gas emissions as a function of ethanol carbon intensity (g-$CO_2$-eq/MJ-Ethanol). Typical ranges for ethanol produced from lignocellulosic residues, sugar cane, and corn grain are shown on top of the figure. Dashed lines correspond to the range of carbon intensities that could be obtained if $CO_2$ capture at the fermentation outlet is implemented.

## Conflicts of interest

"There are no conflicts to declare".

## Author Contributions

Juan-Manuel Restrepo-Flórez: conceptualization, data curation, formal analysis, investigation, methodology, software, visualization, writing–original draft. Paolo Cuello-Peñaloza: conceptualization, data curation, formal analysis, investigation, methodology, writing–original draft. Emmanuel Canales: conceptualization, data curation, formal analysis, investigation, methodology, writing–original draft Dustin Witkowski: conceptualization, formal analysis, investigation, methodology, software, writing –original draft. David Rothamer: conceptualization, resources, funding acquisition, supervision, project administration, writing – review & editing. George W. Huber: conceptualization, methodology, resources, funding acquisition, supervision, project administration, writing – review & editing. Christos T. Maravelias: conceptualization, methodology, resources, funding acquisition, supervision, project administration, writing – review & editing.

## Acknowledgements

This material is based upon work supported by the U.S. Department of Energy's Office of Energy Efficiency and Renewable Energy (EERE)

under the Co-Optima program award number E-EE0008480. The views expressed herein do not necessarily represent the views of the U.S. Department of Energy or the United States Government.

## Notes and references

1 IEA, *Global EV Outlook 2021*, 2021.
2 EIA, *Annual energy outlook 2021*, Washington DC, 2021, vol. 2021.
3 N. M. Eagan, M. D. Kumbhalkar, J. S. Buchanan, J. A. Dumesic and G. W. Huber, *Nat. Rev. Chem.*, 2019, **3**, 223–249.
4 V. Smil, *IEEE Spectr.*, 2019, **56**, 22.
5 V. Smil, *IEEE Spectr.*, 2016, 2016.
6 R. A. Dagle, A. D. Winkelman, K. K. Ramasamy, V. Lebarbier Dagle and R. S. Weber, *Ind. Eng. Chem. Res.*, 2020, **59**, 4843–4853.
7 EIA, *Monthly energy review-June 2021*, Washington DC, 2021, vol. 159.
8 DOE, Global ethanol production by country or region, http://www.agri-outlook.org/%0A.
9 Statista, Biodiesel production in Brazil from 2009 to 2021, https://www.statista.com/statistics/877042/brazil-biodiesel-production/.
10 M. Slupska and D. Bushong, *Biofuels, Bioprod. Biorefining*, 2019, **13**, 857–859.
11 S. P. Singh and D. Singh, *Renew. Sustain. Energy Rev.*, 2010, **14**, 200–216.
12 EPA, Overview for Renewable Fuel Standard Program, https://www.macrotrends.net/2538/soybean-oil-prices-historical-chart-data.
13 Corn grain price, https://markets.businessinsider.com/commodities/corn-price.
14 M. Langholtz, B. Stokes and L. Eaton, *2016 billion-ton report: Advancing domestic resources for a thriving bioeconomy*, Oak Ridge, Tennessee, 2016.
15 J. M. Restrepo-Flórez and C. T. Maravelias, *Energy Environ. Sci.*, 2021, 9–19.
16 J. Sun and Y. Wang, *ACS Catal.*, 2014, **4**, 1078–1090.
17 EPA, Overview for Renewable Fuel Standard, https://www.epa.gov/renewable-fuel-standard-program/overview-renewable-fuel-standard.
18 DOE, Biodiesel Income Tax Credit.
19 J. R. Hannon, L. R. Lynd, O. Andrade, P. T. Benavides, G. T. Beckham, M. J. Biddy, N. Brown, M. F. Chagas, B. H. Davison, T. Foust, T. L. Junqueira, M. S. Laser, Z. Li, T. Richard, L. Tao, G. A. Tuskan, M. Wang, J. Woods and C. E. Wyman, *Proc. Natl. Acad. Sci.*, 2019, 201821684.
20 S. Geleynse, K. Brandt, M. Garcia-Perez, M. Wolcott and X. Zhang, *ChemSusChem*, 2018, **11**, 3728–3741.
21 J. Saavedra Lopez, R. A. Dagle, V. L. Dagle, C. Smith and K. O. Albrecht, *Catal. Sci. Technol.*, 2019, **9**, 1117–1131.
22 K. Atsonios, M. A. Kougioumtzis, K. D. Panopoulos and E. Kakaras, *Appl. Energy*, 2015, **138**, 346–366.
23 L. Tao, J. N. Markham, Z. Haq and M. J. Biddy, *Green Chem.*, 2017, **19**, 1082–1101.
24 E. C. Tan, L. J. Snowden-Swan, M. T. Abhijit-Dutta, S. Jones, K. K. Ramasamy, M. Gray, R. Dagle, A. Padmaperuama, Ma. Gerber, A. H. Sahir, L. Tao and Y. Zhang, *Biofuels, Bioprod. Biorefining*, 2016, **11**, 41–66.
25 W.-C. Wang, L. Tao, J. Markham, Y. Zhang, E. Tan, L. Batan, M. Biddy, W.-C. Wang, L. Tao, Y. Zhang, E. Tan, E. Warner and M. Biddy, *Review of biojet fuel conversion technologies-NREL/TP-5100-66291*, 2016.
26 B. C. Klein, M. F. Chagas, T. L. Junqueira, M. C. A. F. Rezende, T. de F. Cardoso, O. Cavalett and A. Bonomi, *Appl. Energy*, 2018, **209**, 290–305.
27 J. T. Crawford, C. W. Shan, E. Budsberg, H. Morgan, R. Bura and R. Gustafson, *Biotechnol. Biofuels*, 2016, **9**, 1–16.
28 M. D. Staples, R. Malina, H. Olcay, M. N. Pearlson, J. I. Hileman, A. Boies and S. R. H. Barrett, *Energy Environ. Sci.*, 2014, **7**, 1545–1554.
29 J. Han, L. Tao and M. Wang, *Biotechnol. Biofuels*, 2017, **10**, 1–15.
30 N. A. Huq, X. Huo, G. R. Hafenstine, S. M. Tifft, J. Stunkel, E. D. Christensen, G. M. Fioroni, L. Fouts, R. L. McCormick, P. A. Cherry, C. S. McEnally, L. D. Pfefferle, M. R. Wiatrowski, P. T. Benavides, M. J. Biddy, R. M. Connatser, M. D. Kass, T. L. Alleman, P. C. St John, S. Kim and D. R. Vardon, *Proc. Natl. Acad. Sci. U. S. A.*, 2019, **116**, 26421–26430.
31 J.-M. Restrepo-Flórez, J. Ryu, D. Witkowski, D. A. Rothamer and C. T. Maravelias, *Energy Environ. Sci.*, , DOI:10.1039/D2EE02202H.
32 J. M. Restrepo-Flórez and C. T. Maravelias, *Future biofuels: A Superstructure-Based Optimization Framework Integrating Catalysis, Process Synthesis, and Fuel Properties*, Elsevier Masson SAS, 2022, vol. 49.
33 J. Heveling, A. van der Beek and M. de Pender, *Appl. Catal.*, 1988, **42**, 325–336.
34 N. M. Eagan, B. J. Moore, D. J. McClelland, A. M. Wittrig, E. Canales, M. P. Lanci and G. W. Huber, *Green Chem.*, 2019, **21**, 3300–3318.
35 USA Patent Office, US 2021/0363085 A1, 2021.
36 J. E. Rorrer, A. T. Bell and F. D. Toste, *ChemSusChem*, 2019, **12**, 2835–2858.
37 J. Yanowitz, M. A. Ratcliff, R. L. McCormick, J. D. Taylor and M. J. Murphy, .
38 L. Ou, H. Cai, H. J. Seong, D. E. Longman, J. B. Dunn, J. M. E. Storey, T. J. Toops, J. A. Pihl, M. Biddy and M. Thornton, *Environ. Sci. Technol.*, 2019, **53**, 12904–12913.
39 J. T. Kozlowski and R. J. Davis, *ACS Catal.*, 2013, **3**, 1588–1600.
40 I. Nezam, J. Zak and D. J. Miller, *Ind. Eng. Chem. Res.*, 2020, **59**, 13906–13915.
41 I. Nezam, L. Peereboom and D. J. Miller, *J. Clean. Prod.*, 2019, **209**, 1365–1375.
42 United States of America, US 2019/0031585 A1, 2019.
43 P. A. Cuello-Penaloza, R. G. Dastidar, S. C. Wang, Y. Du, M. P. Lanci, B. Wooler, C. E. Kliewer, I. Hermans, J. A. Dumesic and G. W. Huber, *Appl. Catal. B Environ.*, , DOI:10.1016/j.apcatb.2021.120984.
44 A. Galadima and O. Muraza, *Ind. Eng. Chem. Res.*, 2015, **54**, 7181–7194.
45 Q. Zhang, J. Dong, Y. Liu, Y. Wang and Y. Cao, *J. Energy Chem.*, 2016, **25**, 907–910.
46 T. Tsuchida, J. Kubo, T. Yoshioka, S. Sakuma, T. Takeguchi and W. Ueda, *J. Catal.*, 2008, **259**, 183–189.
47 H. S. Ghaziaskar and C. C. Xu, *RSC Adv.*, 2013, **3**, 4271–4280.
48 J. Pang, M. Zheng, L. He, L. Li, X. Pan, A. Wang, X. Wang and T. Zhang, *J. Catal.*, 2016, **344**, 184–193.
49 United States of America, US 10669221 B2, 2020.
50 P. A. Cuello-penaloza, J. Chavarrio-Canas, Y. Du, M. P. Lanci, D. A. Maedke, J. A. Dumesic and G. W. Huber, *Appl. Catal. B Environ.*, 2022, **318**, 121821.
51 D. D. Petrolini, N. Eagan, M. R. Ball, S. P. Burt, I. Hermans, G. W. Huber, J. A. Dumesic and L. Martins, *Catal. Sci. Technol.*, 2019, **9**, 2032–2042.
52 J. J. Bravo-Suárez, B. Subramaniam and R. V. Chaudhari, *Appl. Catal. A Gen.*, 2013, **455**, 234–246.

 

53 E. Medina, R. Bringué, J. Tejero, M. Iborra and C. Fité, *Appl. Catal. A Gen.*, 2010, **374**, 41–47.
54 O. V. Larina, K. V. Valihura, P. I. Kyriienko, N. V. Vlasenko, D. Y. Balakin, I. Khalakhan, T. Čendak, S. O. Soloviev and S. M. Orlyk, *Appl. Catal. A Gen.*, 2019, **588**, 1–11.
55 R. J. J. Nel and A. De Klerk, *Ind. Eng. Chem. Res.*, 2009, **48**, 5230–5238.
56 N. P. Makgoba, T. M. Sakuneka, J. G. Koortzen, C. Van Schalkwyk, J. M. Botha and C. P. Nicolaides, *Appl. Catal. A Gen.*, 2006, **297**, 145–150.
57 V. O. Samoilov, D. N. Ramazanov, A. I. Nekhaev, S. V. Egazar'Yants and A. L. Maximov, *Fuel Process. Technol.*, 2015, **140**, 312–323.
58 A. Forestière, H. Olivier-Bourbigou and L. Saussine, *Oil Gas Sci. Technol.*, 2009, **64**, 649–667.
59 J. Skupińska, *Chem. Rev.*, 1991, **91**, 613–648.
60 G. J. P. Britovsek, R. Malinowski, D. S. McGuinness, J. D. Nobbs, A. K. Tomov, A. W. Wadsley and C. T. Young, *ACS Catal.*, 2015, **5**, 6922–6925.
61 C. P. Nicholas, *Appl. Catal. A Gen.*, 2017, **543**, 82–97.
62 J. Q. Bond, D. M. Alonso, D. Wang, R. M. West and J. A. Dumesic, *Science (80-. ).*, 2010, **327**, 1110–1114.
63 C. Flego, M. Marchionna and C. Perego, *Stud. Surf. Sci. Catal.*, 2005, **158 B**, 1271–1278.
64 ASTM D975-20c, *Standard specification for diesel fuel*, 2014.
65 ASTM D4814−14b, *Standard Specification for Automotive Spark-Ignition Engine Fuel*, 2014.
66 B. Linnhoff and E. Hindmarsh, *Chem. Eng. Sci.*, 1983, **38**, 745–763.
67 D. Humbird, R. Davis, L. Tao, C. Kinchin, D. Hsu, A. Aden, P. Schoen, J. Lukas, B. Olthof, M. Worley, D. Sexton and D. Dudgeon, *Process Design and Economics for Biochemical Conversion of Lignocellulosic Biomass to Ethanol: Dilute-Acid Pretreatment and Enzymatic Hydrolysis of Corn Stover*, Golden, Colorado, 2011.
68 F. G. Baddour, L. Snowden-Swan, K. M. Van Allsburg, J. Super, E. Tan, J. Frye, J. White, J. Schaidle, M. Talmadge, J. Hensley and S. Habas, 2018, 1–54.
69 M. Ryberg, M. D. M. Vieira, M. Zgola, J. Bare and R. K. Rosenbaum, *Clean Technol. Environ. Policy*, 2014, **16**, 329–339.
70 N. Von Der Assen, P. Voll, M. Peters and A. Bardow, *Chem. Soc. Rev.*, 2014, **43**, 7982–7994.
71 K. Gerbrandt, P. L. Chu, A. Simmonds, K. A. Mullins, H. L. MacLean, W. M. Griffin and B. A. Saville, *Curr. Opin. Biotechnol.*, 2016, **38**, 63–70.
72 J. A. Obnamia, G. M. Dias, H. L. MacLean and B. A. Saville, *Appl. Energy*, 2019, **235**, 591–601.
73 A. König, L. Neidhardt, J. Viell, A. Mitsos and M. Dahmen, *Comput. Chem. Eng.*, , DOI:10.1016/j.compchemeng.2019.106712.
74 A. König, M. Siska, A. M. Schweidtmann, J. G. Rittig, J. Viell, A. Mitsos and M. Dahmen, *Chem. Eng. Sci.*, , DOI:10.1016/j.ces.2021.116562.
75 Y. Gaston-Bonhomme, P. Petrino and J. L. Chevalier, *Chem. Eng. Sci.*, 1994, **49**, 1799–1806.
76 H. J. Liaw and Y. Y. Chiu, *J. Hazard. Mater.*, 2006, **137**, 38–46.
77 F. A. Carroll, C. Y. Lin and F. H. Quina, *Ind. Eng. Chem. Res.*, 2011, **50**, 4796–4800.
78 F. I. C. Mirante and J. A. P. Coutinho, *Fluid Phase Equilib.*, 2001, **180**, 247–255.
79 A. M. Ferris and D. A. Rothamer, *Fuel*, 2016, **182**, 467–479.
80 Dustin Witkowski and D. A. Rothamer, in *Spring Technical Meeting of The Central States Section of the Combustion Institute,* Detroit, 2022.
81 M. Groendyk and D. Rothamer, *Fuel*, 2017, **194**, 195–210.
82 NDEE, Average corn grain price, https://neo.ne.gov/programs/stats/inf/66.html.
83 International Renewable Energy Agency, *Road Transport: The Cost of Renewable Solutions*, Bonn, 2013.
84 K. Huang, W. Won, K. J. Barnett, Z. J. Brentzel, D. M. Alonso, G. W. Huber, J. A. Dumesic and C. T. Maravelias, *Appl. Energy*, 2018, **213**, 585–594.
85 C. A. S. Hall, J. G. Lambert and S. B. Balogh, *Energy Policy*, 2014, **64**, 141–152.
86 C. A. S. Hall, S. Balogh and D. J. R. Murphy, *Energies*, 2009, **2**, 25–47.
87 R. T. L. Ng and C. T. Maravelias, *Appl. Energy*, 2017, **205**, 1571–1582.
88 L. Wang, M. Xia, H. Wang, K. Huang, C. Qian, C. T. Maravelias and G. A. Ozin, *Joule*, 2018, **2**, 1055–1074.
89 R. T. L. Ng and C. T. Maravelias, *Appl. Energy*, 2017, **205**, 1571–1582.
90 EPA, Lifecycle Greenhouse Gas Results, https://www.epa.gov/fuels-registration-reporting-and-compliance-help/lifecycle-greenhouse- gas-results, (accessed 17 September 2022).
91 C. H. Geissler and C. T. Maravelias, *Appl. Energy*, 2021, **302**, 117539.
92 Z. Huang, G. Grim, J. Schaidle and L. Tao, *Appl. Energy*, 2020, **280**, 115964.
93 S. Kim, X. Zhang, A. D. Reddy, B. E. Dale, K. D. Thelen, C. D. Jones, R. C. Izaurralde, T. Runge and C. Maravelias, *Environ. Sci. Technol.*, 2020, **54**, 10797–10807.
94 M. Wang, J. Han, J. B. Dunn, H. Cai and A. Elgowainy, *Environ. Res. Lett.*, 2012, 045905.